LRRC52 (leucine-rich-repeat-containing protein 52), a testis-specific auxiliary subunit of the alkalization-activated Slo3 channel

Chengtao Yang, Xu-Hui Zeng, Yu Zhou, Xiao-Ming Xia, and Christopher J. Lingle[1]

Department of Anesthesiology, Washington University School of Medicine, St. Louis, MO 63110

Edited by Richard W. Aldrich, University of Texas, Austin, TX, and approved October 20, 2011 (received for review July 8, 2011)

KSper, a pH-dependent K^+ current in mouse spermatozoa that is critical for fertility, is activated by alkalization in the range of pH 6.4–7.2 at membrane potentials between −50 and 0 mV. Although the KSper pore-forming subunit is encoded by the *Slo3* gene, heterologously expressed Slo3 channels are largely closed at potentials negative to 0 mV at physiological pH. Here we identify a Slo3-associating protein, LRRC52 (leucine-rich repeat-containing 52), that shifts Slo3 gating into a range of voltages and pH values similar to that producing KSper current activation. Message for LRRC52, a homolog of the Slo1-modifying LRRC26 protein, is enriched in testis relative to other homologous LRRC subunits and is developmentally regulated in concert with that for Slo3. LRRC52 protein is detected only in testis. It is markedly diminished from *Slo3*$^{-/-}$ testis and completely absent from *Slo3*$^{-/-}$ sperm, indicating that LRRC52 expression is critically dependent on the presence of Slo3. We also examined the ability of other LRRC subunits homologous to LRRC26 and LRRC52 to modify Slo3 currents. Although both LRRC26 and LRRC52 are able to modify Slo3 function, LRRC52 is the stronger modifier of Slo3 function. Effects of other related subunits were weaker or absent. We propose that LRRC52 is a testis-enriched Slo3 auxiliary subunit that helps define the specific alkalization dependence of KSper activation. Together, LRRC52 and LRRC26 define a new family of auxiliary subunits capable of critically modifying the gating behavior of Slo family channels.

The pore-forming subunit of the sperm-specific alkalization-activated K^+ current, termed KSper (1), is encoded by the *Slo3* gene (2). Deletion of the *Slo3* gene abolishes pH-sensitive K^+ current in testicular (3) and epididymal sperm (4) and results in infertile male mice (3, 4). However, the properties of Slo3 channels studied in heterologous systems (5, 6) differ from those of native KSper currents (1, 4). Whereas native KSper current is appreciably activated at pH 7.0 at potentials negative to 0 mV (1), Slo3 current studied in *Xenopus* oocytes exhibits little activation at pH 7.0 even up to +100 mV (4). This suggests that some unidentified regulatory components of Slo3 channels may contribute to native KSper current.

Recently, a new regulatory subunit of Slo1 BK-type channels, LRRC26, has been shown to markedly shift gating of Slo1, even in the absence of Ca^{2+}, in prostate tumor cells (7). LRRC26 is one of a large number of LRRC (leucine-rich-repeat-containing) proteins, of which there are multiple superfamilies (8). LRRC26 belongs to an extracellular leucine-rich-repeat–only (Elron) cluster, which includes five other LRRC proteins: LRRC38, LRRC52, LRRC55, LRTM1 and LRTM2. Elron cluster members are all predicted to contain a single transmembrane segment with an N-terminal signal peptide resulting in extracellular localization of the LRR domain and a short cytoplasmic C-terminal tail containing a short stretch of acidic residues. Despite shared organization of leucine-rich-repeats among Elron family LRRC proteins, additional amino acid homology is modest. However, their common structural organization suggests they may share structurally similar interaction partners. Here we have evaluated the possibility that a testis-specific, Elron-family LRRC protein may interact with the Slo1 homolog, Slo3.

Our results establish that, of the Elron family members, LRRC52 protein is a candidate for a testis-specific, Slo3 interacting partner. The *lrrc52* message and its encoded protein are enriched in testis. The developmental time-course of *lrrc52* expression mirrors that of *Slo3*. Currents arising from coexpression of Slo3 and LRRC52 in *Xenopus* oocytes exhibit pH- and voltage-dependence more similar to native KSper currents than for Slo3 alone. Furthermore, deletion of Slo3 strikingly decreases LRRC52 protein abundance in mouse testis and abolishes the presence of LRRC52 in sperm. We propose that LRRC52 is a testis-specific, Slo3 auxiliary subunit that is essential for the activation of KSper current at physiological membrane potentials and pH. The results support the possibility that at least some Elron proteins may constitute a family of unique interacting partners for Slo family channels.

Results

***lrrc52* Is the Most Abundantly Expressed Elron Cluster Gene in Mouse Testis.** The *Slo3* gene is selectively expressed in mouse testis (2, 4). To assess whether an Elron family LRRC protein (8) might be a Slo3 channel auxiliary subunit, we determined the expression in mouse testis of the six Elron cluster members along with two testis-expressed non-Elron *lrrc* messages, *lrrc6* and *lrrc28* (Fig. 1*A*). Of the Elron genes, only *lrrc52* had absolute expression levels comparable to *Slo3*, while mRNA abundance of other Elron members was at least 10-fold lower than for *Slo3* and *lrrc52*. Consistent with the biogps database (http://biogps.gnf.org), messages for *lrrc6* and *lrrc28* were also abundant in testis, but both define proteins without homology with Elron subunits (8). We also compared the time course of *lrrc52* and *Slo3* gene expression in testis from postpartum day 3 to day 150. Developmental expression of *kcnbm4*, which encodes the BK β4 auxiliary subunit, was also defined, since β4 was proposed as a potential interacting partner of Slo3 in testis (9). *Slo1* was included as a control. The results revealed that *lrrc52* and *Slo3* genes share very similar expression time courses, being very low before P25, exhibiting pronounced enhancement between P25 and P30, and then persisting at a constant high level from P30 through P150 (Fig. 1*B*). In contrast, *Slo1* message levels remained low through all 150 d postpartum while *kcnmb4* gene expression increased modestly as early as P20.

We next tested the ability of Slo3 and HA-tagged LRRC52 subunits to coassemble, using coimmunoprecipitation (Co-IP)

Author contributions: C.Y., X.-H.Z., and C.J.L. designed research; C.Y., X.-H.Z., Y.Z., and X.-M.X. performed research; C.Y., X.-H.Z., Y.Z., and C.J.L. analyzed data; and C.Y. and C.J.L. wrote the paper.

The authors declare no conflict of interest.

This article is a PNAS Direct Submission.

[1]To whom correspondence should be addressed. E-mail: clingle@morpheus.wustl.edu.

This article contains supporting information online at www.pnas.org/lookup/suppl/doi:10.1073/pnas.1111104108/-/DCSupplemental.

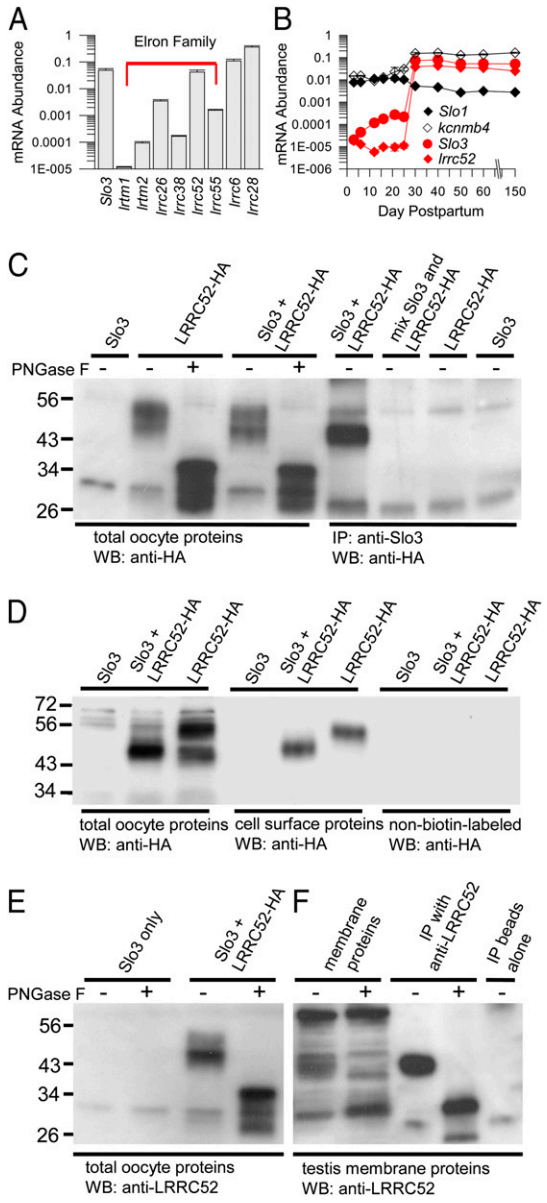

Fig. 1. LRRC52 is a candidate auxiliary subunit of Slo3. (*A*) Relative abundance of message for all Elron-family LRRC subunits (LRTM1, LRTM2, LRRC26, LRRC38, LRRC52, and LRRC55) along with two other testis-associated LRRC proteins (LRRC6 and LRRC28) was determined using RT-qPCR. All estimates were normalized to the level of *β-actin* message. All determinations were from three separate RNA preparations, each run in triplicate. (*B*) Message for *Slo3*, *Irrc52*, *Slo1*, and *kcnmb4* were determined from mouse testis for different days postpartum. Each point is the mean of estimates from three separate animals, each run in triplicate. (*C*) Slo3 and HA-tagged LRRC52 coassemble in *Xenopus* oocytes. Batches of oocytes were injected with cRNA for either Slo3 alone, LRRC52-HA alone, or both together. The left five lanes show Western blotting of total oocyte proteins and staining with anti-HA antibody. HA-tagged LRRC52 protein is observed at ∼47–55 kDa when glycosylated (PNGase F–) and at ∼36 kDa following deglycosylation (PNGase F+). In the four right lanes, oocyte proteins were first immunoprecipitated with anti-Slo3. Anti-Slo3 only pulls down LRRC52-HA in the lane corresponding to coexpression of Slo3 and LRRC52. (*D*) Oocytes were separately incubated with or without biotin. Lanes 1–3 show anti-HA-stained labeled proteins from total oocyte proteins for oocytes injected with Slo3 alone, Slo3+LRRC52-HA, and LRRC52-HA alone. Lanes 4–6 show biotinylated proteins pulled down by streptavidin for sets of oocytes injected with Slo3 alone (lane 4), Slo3+LRRC52-HA (lane 5), and LRRC52-HA alone (lane 6), after staining with anti-HA. The right three lanes show blotting with anti-HA for proteins pulled down by streptavidin from nonbiotin labeled oocytes. (*E*) A polyclonal LRRC52 Ab identifies the LRRC52-HA protein in oocytes. To confirm validity of a polyclonal LRRC52 Ab, Slo3 was expressed with and without LRRC52-HA in oocytes. Oocytes expressing Slo3 alone exhibit minimal nonspecific bands either with or without glycanase treatment (lanes 1 and 2). For oocytes expressing both Slo3 and LRRC52-HA, the anti-LRRC52 Ab identified bands identical to those revealed by anti-HA Ab under both glycosylated (lane 3) and deglycosylated (lane 4) conditions. (*F*) LRRC52 protein is present in mouse testis. Anti-LRRC52 Ab labels multiple bands in total testis membrane proteins (lanes 1 and 2). However, the Ab identifies a 45-kDa band in glycosylated proteins (lane 1), which is absent following glycanse treatment (lane 2), with an increased density at ∼33 kDa. When testis membrane proteins are first immunoprecipitated with anti-LRRC52 antibody, the anti-LRRC52 Ab revealed a prominent glycosylated band at 45 kDa (lane 3) and a strong band at ∼33 kDa (with a minor 24-kDa band) following deglycosylation (lane 4). IP with IP beads alone lacking the LRRC52 Ab identified a nonspecific band at 26 kDa (lane 5) also seen in all other lanes.

methods following coexpression in *Xenopus* occytes. Total LRRC52 protein levels in oocytes were similar in the presence and absence of Slo3 (Fig. 1*C*). In total oocyte proteins, the HA antibody labeled two protein bands, one at ∼47 kDa and one at ∼54 kDa (Fig. 1*C*). Following deglycosylation, these bands disappeared, revealing a main band around 36 kDa and a weaker band around 26 kDa. Based on the amino acid sequence, mouse LRRC52 is predicted to be a glycoprotein with 4 *N*-linked glycosylation sites. Its molecular weight after deglycosylation is predicted to be 35 kDa and, with the added HA-tag, 38 kDa. The 47 kDa and 54 kDa bands in total oocyte proteins in Fig. 1*C* likely represent multiple glycosylated forms of LRRC52-HA, while the 36 kDa protein in PNGase F(+) lanes corresponds to deglycosylated LRRC52-HA with N-terminal signal peptide removed. The weak 26 kDa protein may be a degraded LRRC52-HA peptide. Coassociation of Slo3 and LRRC52 was demonstrated in oocytes coinjected with both subunits (Slo3+LRRC52-HA) but not in negative controls (oocytes injected with Slo3 only, oocytes with LRRC52-HA only) (Fig. 1*C*). When proteins from oocytes separately injected with LRRC52 and Slo3 were mixed, no coassembly between LRRC52 and Slo3 was observed. The anti-Slo3 Ab appeared to preferentially pull down the smaller ∼47 kDa form of HA-tagged LRRC52 suggesting that Slo3 may specifically interact with a particular form of LRRC52.

As a further probe of Slo3 and LRRC52 interactions, we used biotinylation to identify cell surface HA-tagged LRRC52 expressed with or without Slo3 (Fig. 1*D*). For oocytes expressing LRRC52-HA alone, only the larger ∼54-kDa LRRC52 band appeared in the cell surface proteins, while when LRRC52-HA was coexpressed with Slo3, the smaller ∼47-kDa form of LRRC52 was preferentially found in the surface membrane (Fig. 1*D*). In some samples from oocytes expressing LRRC52-HA + Slo3, a weak ∼54-kDa LRRC52 band was also observed in the plasma membrane. This may reflect some fraction of LRRC52 which appears in the surface membrane that is not associated with Slo3. Together these results (Fig. 1 *C* and *D*) show that Slo3 specifically coassembles with a smaller molecular weight form of LRRC52 and that Slo3 is required for the smaller LRRC52 form to appear in surface membrane.

To test for the presence of LRRC52 protein in native mouse testis, a polyclonal rabbit anti-LRRC52 Ab was generated. The anti-LRRC52 Ab successfully identified the glycosylated and deglycosylated bands of LRRC52-HA in oocyte proteins (Fig. 1*E*). In testis membrane proteins, the anti-LRRC52 Ab labeled multiple protein bands (Fig. 1*F*) both without and with PNGase F treatment. However, only a single prominent band around 45 kDa disappeared with deglycosylation, with a band around 33 kDa being enriched following PNGase F treatment. Thus, of all testis proteins labeled with the anti-LRRC52 Ab, only one appears to be glycosylated and, following deglycosylation, migrates

close to the predicted molecular weight of LRRC52 (with signal peptide cleaved). Following enrichment of candidate LRRC52 protein by sequential immunoprecipitation and Western blot with anti-LRRC52 antibody, the 45-kDa protein became the only prominent band in the IP products (Fig. 1*F*). As expected, with PNGase F treatment, the band shifted to ~33 kDa with a weak secondary band at 24 kDa. The glycosylated 45-kDa protein in native testis proteins has four properties consistent with LRRC52: it is a membrane protein, it is a glycosylated protein, following deglycosylation it runs with a molecular weight appropriate for LRRC52, and it is recognized by an Ab that recognizes heterologously expressed LRRC52. It should also be noted that the glycosylated molecular weight of the testis LRRC52 corresponds closely to that of the 47-kDa smaller form of LRRC52 expressed in oocytes and which selectively associates with Slo3. We conclude that both *lrrc52* message and LRRC52 protein are expressed in mouse testis and LRRC52 is a candidate functional partner of Slo3 channel in testis. Although coassembly between Slo3 and LRRC52 was readily detected in oocytes (Fig. 1*C*), we were unable to obtain successful Co-IP of Slo3 and LRRC52 in testis proteins, despite the use of multiple solubilization conditions.

LRRC52 Shifts Slo3 Gating to More Negative Potentials at a Given pH. We next tested the ability of LRRC52 to modify Slo3 gating behavior using heterologous expression of LRRC52 with Slo3 in *Xenopus* oocytes. Currents arising from Slo3 channels with or without LRRC52 were examined over voltages from −120 to +240 mV at pH values from 6.0 to 9.0 (Fig. 2*A* and Fig. S1). Conductance-voltage (GV) relationships were determined for Slo3+LRRC52 currents and were normalized to the maximum values recorded at pH 9.0 and +240 mV (Fig. 2*B*). Similarly, GV curves for Slo3 alone were generated at pH up to 9.0. Compared with GV curves from Slo3 alone, the normalized G–V relationship from oocytes with Slo3+ LRRC52 exhibited a substantial leftward shift and Slo3+LRRC52 currents were activated at pH 7.0 at membrane potentials negative to 0 mV (Fig. 2*B* and Fig. S1).

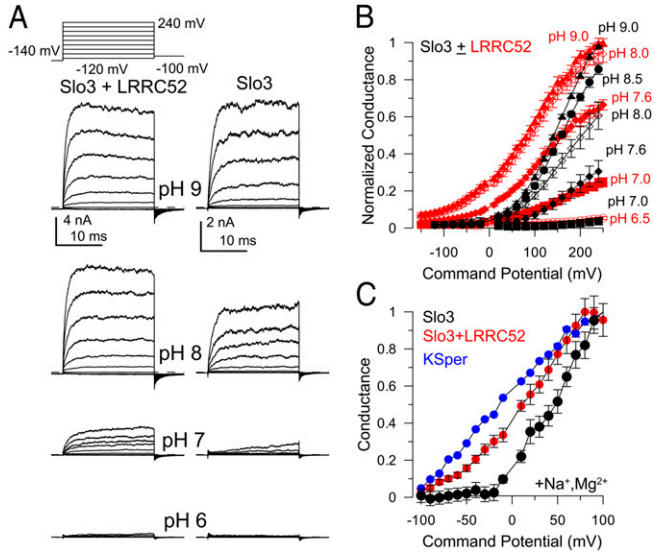

Fig. 2. LRRC52 shifts Slo3 channel gating making it more similar to KSper current in sperm. (*A*) Coexpression of Slo3 with LRRC52 resulted in activation of current at lower pH and membrane voltages. (*Left*) Currents in inside-out patches from oocytes expressing both Slo3 and LRRC52 were elicited with the indicated voltage-protocol and cytosolic pH. (*Right*) Currents from Slo3 alone are displayed. (*B*) GV curves (normalized to the conductances at +250 mV and pH 8.0) are shown for Slo3 alone (black) and Slo3+LRRC52 (red). For Slo3, test solutions were pH 6.5 (not plotted), 7.0, 7.6, 8.0, 8.5, and 9.0. For Slo3+LRRC52, pH was 6.0 (not plotted), 6.5, 7.0, 7.2 (not plotted), 7.6, 8.0, and 9.0. (*C*) GV curves normalized to the estimate at +80 mV are plotted for native mouse sperm KSper (blue) isolated by clofilium-subtraction (4), Slo3 (black), and Slo3+LRRC52 (red). The recording conditions used symmetric K^+ solutions with a cytosolic solution also containing 15 mM Na^+ and 3 mM Mg^{2+}, typically used in sperm recordings.

At +240 mV, pH 8.5 produces near maximal activation of Slo3 conductance (5), although single Slo3 channels open to relatively modest Po (~0.3) at these conditions (6). Examination of single Slo3+LRRC52 channels at +240 at pH 8.0 (where additional increases in pH have no effect) revealed similar Po estimates near 0.3 (Fig. S2), which was also confirmed in macroscopic current patches using analysis of current variance. This similarity between Slo3 and Slo3+LRRC52 in single channel Po at +240 and at a pH producing near maximal activation requires that the enhancement of relative conductance at lower pH and voltages observed for Slo3+LRRC52 results from a shift in channel gating properties and not an increase in channel number or maximal Po. Because of similarity in single channel Po at conditions approaching maximal activation, this allowed renormalization of the GV curves in terms of absolute conductance values (Fig. S3). Evaluation of such GV curves in terms of the Horrigan-Aldrich model used to describe allosteric gating of both Slo1 (10) and Slo3 (5) suggests that the association of LRRC52 with Slo3 produces strong effects on the constant describing the channel closed-open equilibrium (Fig. S3), with smaller effects on other allosteric constants (see *SI Materials and Methods* for details).

KSper currents in native sperm are typically studied with cytosolic solutions containing 15 mM Na^+ and 3 mM Mg^{2+} (1). These identical solutions result in voltage-dependent inhibition of Slo3 channels (4) thereby increasing relative Slo3 current at more negative potentials, but still insufficient to explain the apparent KSper activation at negative pH and voltage. Here, when Slo3 and Slo3+LRRC52 currents were compared at pH 8.0 with cytosolic salines containing Na^+ and Mg^{2+} (4), the Slo3+LRRC52 conductance at pH 8.0 exhibited a dependence on voltage that approached that of native clofilium-isolated KSper current in mouse sperm (Fig. 2*C*). However, although Slo3+LRRC52 better approximates native KSper current than Slo3 alone, the combination of Slo3+LRRC52 does not appear to fully account for the activation at low pH and negative voltages that is observed for native KSper current.

Deletion of the *Slo3* Gene Abolishes LRRC52 Protein in Cauda Epididymal Sperm. LRRC52, Slo3, and KCNMB4 protein levels were compared in WT, $Slo3^{-/-}$ and $kcnmb4^{-/-}$ mice using Western blotting, both in total testis membrane proteins and in immunoprecipitated proteins. Compared with WT testis, LRRC52 protein levels were markedly reduced in $Slo3^{-/-}$ testis but normal in $kcnmb4^{-/-}$ testis (Fig. 3*A*). Although the anti-LRRC52 Ab recognizes multiple nonspecific bands in testis membrane protein samples, IP with anti-LRRC52 resolved the specific LRRC52 protein band allowing comparison of relative protein abundance in the three mouse strains (Fig. 3*B*). The density of the LRRC52 band in each mouse strain (WT, $Slo3^{-/-}$, $kcnmb4^{-/-}$) was quantified and normalized to the WT value. For three independent experiments, the ratios of the LRRC52 levels were, for $Slo3^{-/-}$: WT, 0.17 ± 0.05 and, for $kcnmb4^{-/-}$: WT, 1.09 ± 0.05. In contrast, the ratio of KCNMB4 protein was, for $Slo3^{-/-}$:WT, 1.19 ± 0.33.

Slo3, LRRC52, KCNMB4 protein levels in cauda epididymal sperm were also compared in WT and $Slo3^{-/-}$ animals. The polyclonal Slo3 Ab identified an ~120 kDa in WT caudal epididimal sperm proteins, but not from $Slo3^{-/-}$ (Fig. 3*C*). Using the anti-LRRC52 antibody, WT sperm proteins contained a 45-kDa protein band which shifted to bands of 33 kDa and a weak 24 kDa following deglycosylation (Fig. 3*C*). In similarly prepared proteins from $Slo3^{-/-}$ sperm, there was no detectable band either

PHYSIOLOGY

in untreated or PNGase F-treated samples. No KCNMB4 protein could be detected in sperm proteins under conditions which readily identified the other two proteins, and which had revealed KCNMB4 protein in testis membrane proteins. RT-qPCR confirmed that *lrrc52* message was identical in WT and *Slo3*$^{-/-}$ testis (Fig. 3*D*), suggesting that transcriptional regulation is not responsible for loss of LRRC52 protein in *Slo3*$^{-/-}$ sperm. Gene expression in all negative controls (−RT) was undetectable. The decreased LRRC52 protein in *Slo3*$^{-/-}$ testis suggests that Slo3 protein may be required to stabilize LRRC52 in native tissue and that loss of LRRC52 occurs when it is not properly assembled with Slo3. The apparently complete absence of LRRC52 in Slo3 null sperm indicates that the presence of LRRC52 in mature sperm depends entirely on the presence of Slo3.

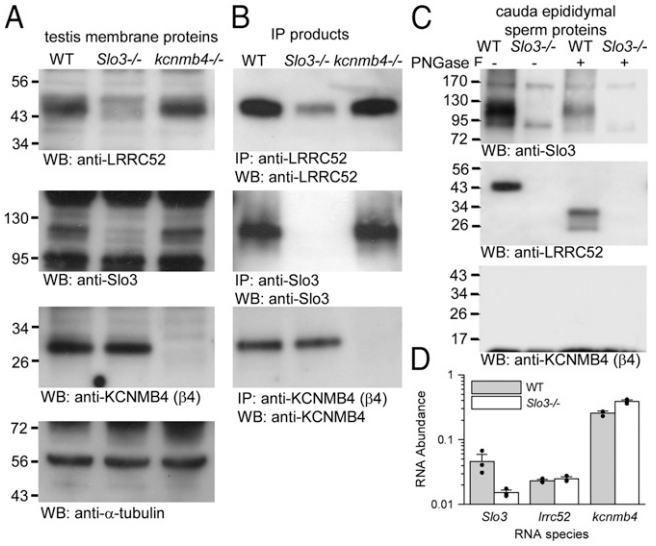

Fig. 3. LRRC52 is absent in *Slo3* null sperm. (*A*) Protein levels of LRRC52, Slo3 and KCNMB4 were compared in WT, *Slo3*$^{-/-}$ and *kcnmb*$^{-/-}$ mouse testis. Fifty micrograms of testis membrane proteins from each mouse strain was loaded in each well to examine target proteins by Western blotting. On the bottom, anti–α-tubulin was used to document comparable loading amounts from each sample. In the first row, proteins were blotted with anti-LRRC52 antibody revealing reduced LRRC52 protein in *Slo3*$^{-/-}$ testis. In the second row, anti-Slo3 Ab labeled multiple bands, but a band of ~120 kDa was absent in the *Slo3*$^{-/-}$ testis. In the third row, anti-KCNMB4 Ab labeled a 28-kDa band in WT and *Slo3*$^{-/-}$ testis proteins, but not in proteins from *kcnmb4*$^{-/-}$ mice. (*B*) Total testis membrane protein samples as in A were first subjected to a round of immunoprecipitation. In the first row, IP with anti-LRRC52 Ab enriched the 45-kDa LRRC52 protein in WT and *kcnmb4*$^{-/-}$ testis. This band is reduced to less than 20% in the *Slo3*$^{-/-}$ proteins. In the second row, IP with anti-Slo3 Ab resulted in enrichment of the Slo3 band in WT and *kcnmb4*$^{-/-}$ testis proteins, but a complete absence of signal from *Slo3*$^{-/-}$ proteins. In the third row, IP with anti-KCNMB4 Ab enriches the KCNMB4 band in WT and *Slo3*$^{-/-}$ testis proteins, with no band in the *kcnmb4*$^{-/-}$ proteins. For separation of IP products, anti-LRRC52 IP product (prepared from 0.3 mg testis membrane proteins of each mouse strain), anti-Slo3 IP product (prepared from 2.5-mg testis membrane proteins) and anti-KCNMB4 IP product (prepared from 1-mg testis membrane proteins) were respectively loaded in the lanes of SDS/PAGE gel. Protein abundance for target protein bands was analyzed with the use of ImageJ software and values were averaged from three independent experiments. (*C*) Slo3, LRRC52, and β4 were compared in proteins isolated from caudal epididymal sperm from WT and *Slo3*$^{-/-}$ mice. One microgram of sperm protein, prepared from about 2×10^5 cauda epididymal sperm, was loaded in each well for Western blotting. The experiment was repeated thrice from separate animals. (*Top*) Samples were blotted with anti-Slo3 polyclonal Ab, revealing a band in WT samples at about 120 kDa. (*Middle*) Samples show robust presence of LRRC52 in WT, but not Slo3$^{-/-}$ samples. (*Bottom*) Samples show the complete absence of detectable β4 protein. (*D*) mRNA abundances of *lrrc52*, *Slo3* and *kcnmb4* were compared in WT and *Slo3*$^{-/-}$ testis by RT-qPCR. Message levels were normalized to the level of *β-actin* message. All determinations were from three separate animals (filled circles), each run in triplicate.

LRRC52 Is Selectively Enriched in Testis. We next asked whether LRRC52 exhibits a tissue specificity appropriate to a selective role as a Slo3-associated protein. mRNA abundance of *lrrc52* was determined for 18 mouse tissues (Fig. 4*A*). The *lrrc52* message in testis was at least 10-fold higher than for any other tested tissue. Possible weak expression was also observed in kidney, ventricle, spinal cord and skeletal muscle. This result is consistent with EST profiles in the National Center for Biotechnology Information database (http://www.ncbi.nlm.nih.gov/UniGene/ESTProfileViewer.cgi?uglist=Mm.159799) which reveals weak *lrrc52* expression primarily in mouse testis and kidney. We also compared the relative abundance of *lrrc26* and *lrrc55* message among the same set of tissues (Fig. S4) and found that both exhibited a much broader distribution than observed for *lrrc52*.

Using the anti-LRRC52 Ab, the relative abundance of LRRC52 protein was compared in Western blots among different tissues, including kidney, heart, skeletal muscle and spinal cord. Cerebral cortex was included as a negative control. At comparable levels of protein loading, no LRRC52 protein was identified in any of the tested tissues except testis (Fig. 4*B*), indicating that LRRC52 protein may be restrictively expressed in testis, similar to Slo3 protein. Bands that appeared in Western blots in cortex and kidney could be excluded as candidate LRRC52 bands, since they did not shift to the size expected for deglycosylated LRRC52 following treatment with PNGase F.

Other Elron Cluster Members also Interact with Slo3 in Oocytes but Are Less Effective at Shifting Slo3 Channel Gating. We also tested the ability of other LRRC subunits to influence Slo3 activation. Although no other LRRC subunit produced the pronounced leftward shift in Slo3 activation observed with LRRC52, LRRC26

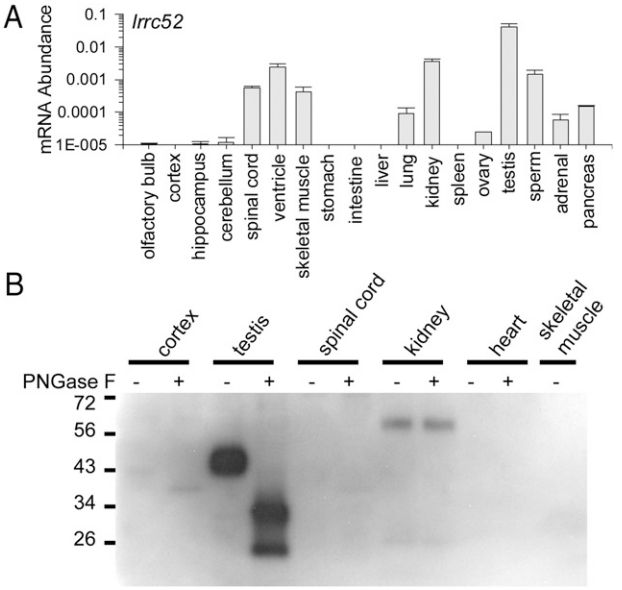

Fig. 4. LRRC52 protein is enriched in testis. (*A*) *lrrc52* message levels were examined in a variety of mouse tissues by RT-qPCR and normalized to the level of *β-actin* message. All determinations were from 3 separate RNA preparations each run in triplicate. (*B*) Following initial IP with anti-LRRC52 Ab, membrane proteins from several mouse tissues were blotted with anti-LRRC52 Ab for both glycosylated (–) and deglycosylated (+) conditions. In each lane, the IP products loaded in the gel were produced from 0.5-mg initial membrane proteins from each tissue.

and LRRC38 produced modest alterations in the resulting currents (Fig. S5*A*). Following normalization of GV curves at pH 8.0, GV curves both for Slo3+LRRC26 and Slo3+LRRC38 exhibited less inhibition at pH 7.6 and pH 7.0 than for Slo3 alone. However, in contrast to LRRC52, LRRC26 and LRRC38 failed to enhance activation of Slo3 currents at membrane potentials negative to 0 mV. The other tested Elron subunits, LRRC55, LRTM1, and LRTM2 did not alter Slo3 gating (Fig. S5*B*). Similarly, the non-Elron subunits, LRRC6 and LRRC28, had no effect (Fig. S6).

The absence of effects of some LRRC subunits on Slo3 currents might arise either from lack of subunit expression or failure to assemble with Slo3. The ability of HA-tagged LRRCs to express and coassemble with Slo3 was therefore examined. For each LRRC subunit, we determined: (*i*) HA-tagged LRRC subunit expression in total oocyte protein (Fig. S5*C*), (*ii*) the ability of anti-Slo3 Ab to pull down HA-tagged LRRC subunits from total oocyte proteins (Fig. S5*D*), and (*iii*) Slo3 subunit expression in the same batch of oocyte proteins (Fig. S5*E*). Because all eight tested LRRC proteins except LRRC28 are predicted to be glycoproteins (Table S1), the observed molecular weights (Fig. S5*C*) were somewhat higher than those predicted directly from their amino acid sequences. LRTM1, LRTM2, LRRC26, LRRC52, LRRC55, and LRRC6 were all abundantly expressed in oocytes (Fig. S5*C*), but only LRTM2, LRRC26 and LRRC52 showed strongly positive Co-IP with Slo3 (Fig. S5*D*). LRRC38 and LRRC55 exhibited only weak coassembly with Slo3. Co-IP between Slo3 protein and LRTM1, LRRC6 or LRRC28 appeared to be negative. Thus, five of the Elron family members, LRTM2, LRRC26, LRRC38, LRRC52 and LRRC55, are competent to interact with Slo3 protein. LRTM1, if it can coassemble with Slo3, appeared to do so much more weakly than for all of the other Elron members. For the non-Elron proteins, LRRC6 and LRRC28, coassembly with Slo3 was not observed, although expression of LRRC28 in oocytes was rather low. The Co-IP data are consistent with the functional results that LRRC52, LRRC26 and LRRC38 interact with Slo3 channels in oocytes.

Discussion

Previous work has demonstrated that Slo3 is an ion channel pore-forming subunit responsible for alkalization-activated KSper current in corpus epididymal sperm (4). However, a critical difference between sperm KSper current and heterologously expressed Slo3 current is that, unlike KSper, Slo3 channel was not appreciably activated at potentials negative to 0 mV and at pH less than 7.2 (5). This suggested that additional regulatory subunits may be required for normal physiological function. Although the BK channel β4 subunit (KCNMB4) enhances Slo3 channel cell surface expression in oocytes (9), it does not shift the alkalization-dependence of Slo3 gating. Here, the present results establish that LRRC52 is a testis-enriched membrane protein that associates with Slo3 and, when coassembled with Slo3, produces alkalization-activated channels with properties that more closely resemble those of KSper current in mouse sperm. The ability of LRRC52 to enhance Slo3 gating was attributed primarily to an effect on the intrinsic closed-open equilibrium constant of Slo3 gating. Although Co-IP of Slo3 and LRRC52 protein was not observed from native tissues, several results strongly argue that LRRC52 is a critical partner of Slo3 channel in sperm. First, message for LRRC52 and Slo3 share a similar developmental expression time course. Second, expression of both LRRC52 and Slo3 proteins appear to be primarily restricted to testis. Third, the presence of LRRC52 in testis and most notably in sperm is absolutely dependent on the presence of Slo3 in sperm. Fourth, currents from LRRC52+Slo3 coexpression more closely mimic native KSper behavior than Slo3 alone. Overall, the results strongly suggest that LRRC52 is a necessary component of KSper channels in mouse sperm.

That KSper channels may involve a macromolecular complex of several critical protein components shares interesting parallels with various aspects of the sperm-associated CatSper channels (11, 12). Native CatSper channels also appear to arise from multiple distinct subunits, presumably up to four pore-forming CatSper subunits, CatSper1-4 (12), while also requiring auxiliary β-, γ-, and δ-subunits (13–15). For native CatSper channels, KO of any of the four CatSper1-4 subunits results in male infertility and, similarly, KO of CatSper δ also produces infertile male mice. Our observation that LRRC52 subunits are totally absent in *Slo3*$^{-/-}$ sperm is similar to the effects of KO of various CatSper subunits on expression of their interacting partners. For example, in *CatSper1*$^{-/-}$ mice, CatSper δ (14) and CatSper β (13) protein is absent from sperm. Such results are taken to support the idea that these proteins are intimate partners of CatSper1-4 in the formation of the functional CatSper channel. Similarly, the absence of LRRC52 protein in sperm from *Slo3*$^{-/-}$ mice supports the idea that LRRC52 is intimately involved with Slo3 subunits and KSper channels.

What might be the expected consequences of LRRC52 deletion? We imagine two possibilities, both of which would result in infertile male mice. First, *lrrc52* KO may result in sperm with an alkalization-activated current similar to the Slo3 current recorded in oocytes. Based on the weak activation of Slo3 under conditions normally present in sperm, we would therefore expect that *lrrc52*$^{-/-}$ male would be infertile. Alternatively, in native sperm, it may be the case that, in the absence of LRRC52 protein, Slo3 itself may not express, thereby also resulting in reproductive abnormalities. We predict that LRRC52 is an essential component of normal mouse male reproductive function and that KO of the *lrrc52* gene should essentially mimic all of the deficits in sperm function associated with Slo3 KO. Might there remain other unidentified participants in native KSper channels? The properties of Slo3+LRRC52 currents may still not fully account for activation of KSper at the lowest pH we have examined. As such, we cannot exclude that other components of KSper remain to be identified.

Another important aspect of this work is that LRRC52 is now the second Elron subfamily member found to interact with Slo family pore-forming subunits. In the first case, LRRC26 was shown to produce a strong negative shift in Slo1 gating in prostate cancer cells and LRRC26 may participate in Slo1 channels in other tissues (7). To our knowledge nothing is known about potential functions of the other Elron members, LRTM1, LRTM2, LRRC38, and LRRC55. Our results establish that at least some of these subunits are competent to associate with Slo3 and perhaps Slo1. It is natural to wonder whether some Elron subunits might play a role in the regulation of other ion channels, perhaps the less-studied Na^+ regulated Slo2.1 and Slo2.2 channels (16, 17) that share some general structural similarity with Slo1 and Slo3 (18).

Taken together, this work suggests that LRRC52 is a Slo3 channel auxiliary subunit in mouse sperm critical for definition of the alkalization-dependence of native KSper current. Furthermore, the results identify Elron LRRC proteins, or at least a subset of them, as a family of unique auxiliary subunits of Slo family pore-forming K^+ channels.

Materials and Methods

Animal Husbandry and Procedures. All animal husbandry and experimental procedures were approved by and performed in accordance with guidelines of the Washington University School of Medicine Animal Care and Use Committee.

Preparation of Constructs. LRRC Elron family subunits, along with LRCC6 and LRCC28 (Table S2), were subcloned into oocyte expression vector pXMX

using PCR on EST clones obtained from Open Biosystems (mLRRC26, BI108309; mLRRC38, BC129963; mLRRC52, CB953430; hLRRC55, BC150572; mLRTM1, BC145990; hLRTM2, BC129997; mLRRC6, BC046277; mLRRC28, BU946312). The HA- and His-tagged constructs were generated by overlapping PCR to insert HA- and His-tags (GGYPYDVPDYAGGHHHHHHHHGG) into the C-termini of LRRC proteins (mLRRC26 at position 331 between EDA and GSP; mLRRC38 at position 425 between CAP and NKD; mLRRC52 at position 293 between SRF and ANQ; hLRRC55 at position 333 between RWS and KAS; mLRTM1 at position 345 between EKM and GSK; hLRTM2 at position 354 between LMG and DPE; mLRRC6 at position 497 between STI and VQE; mLRRC28 at position 359 between TQC and LRT). cRNAs were in vitro synthesized after being linearized with MluI.

Electrophysiology. Recordings of macroscopic and single channel currents used inside-out patches from constructs expressed in *Xenopus* oocytes with additional details provided in *SI Materials and Methods*.

RNA Extraction and Quantitative RT-PCR. Total RNA from mouse tissue was isolated using the RNeasy Plus Mini Kit (Qiagen) following the manufacturer's recommendations and then treated with the DNA-free Kit (AM1906; Applied Biosystems) to remove genome DNA. cDNA was synthesized using the Retroscript Kit (AM1710; Applied Biosystems). Roche random hexamer was applied in reverse transcription. For the negative control groups, all components except the reverse transcriptase MMLV-RT were included in the reaction mixtures. Real-Time PCR was performed with specific primers (Table S2) and Power SYBR Green PCR Master Mix (Applied Biosystems) under reaction conditions identical to that described previously (9). The slopes of primer efficiency equation for primer pairs used in this study were between −3.1 and −3.6, giving reaction efficiencies between 90% and 110%, which are typically acceptable for quantitative PCR assay. Message levels were normalized to the abundance of *β-actin* message in data analysis. In the *Slo3*$^{-/-}$ mice, exon 27 was deleted. Therefore, primers were designed to detect residual Slo3 message likely to be expressed in the *Slo3*$^{-/-}$ mice (4).

Protein Preparation. Protein preparation methods from mouse tissues, *Xenopus* oocytes and sperm follow standard procedures and are described in the *SI Materials and Methods*.

Immunoprecipitation and Western Blotting. The rabbit anti-LRRC52 antibody (ProSci) was raised to an epitope near the LRRC52 C terminus corresponding to residues NALRTSSGDDTEDETGSRFANQ. For mouse tissue, 12 mg of membrane proteins was used for immunoprecipitation (IP) with rabbit anti-LRRC52 antibody. For oocyte samples, 0.75 mL of oocyte (Slo3 + LRRC) total protein preparation was applied for IP with monoclonal anti-Slo3 antibody (N2/16; Antibodies, Inc.). For oocyte mixing controls, 0.75 mL of oocyte (Slo3) total proteins was mixed together with 0.75 mL of oocyte (LRRC) total proteins for IP. Protein preparation was precleared by incubation with 30 μL Trueblot anti-rabbit Ig or anti-mouse Ig IP beads (eBioscience) in a 4 °C cold room for 1 h, followed by a brief centrifuging at 15,000 × *g* to precipitate the beads. The supernatant was collected and mixed with 10 μg antibody in a 4 °C cold room for 2 h, followed by the addition of 50 μL Trueblot IP beads. The mixture was rocked overnight and then centrifuged briefly to collect the beads. Beads were washed thrice with 1% Triton X-100 lysis buffer and the bound proteins were then eluted with 100 μL SDS loading buffer containing 100 mM DTT. Other details of Western blots were as previously described (4, 9). Antibodies used for Western blotting were rabbit anti-HA antibody (0.8 μg/mL; Santa Cruz), rabbit polyclonal anti-Slo3 antibody (3 μg/mL, ProSci), rabbit anti-LRRC52 antibody (3.75 μg/mL; ProSci.), rabbit anti-KCNMB4 antibody (4 μg/mL; Alomone Lab) and mouse anti-α-tubulin antibody (1 μg/mL; Invitrogen). Secondary antibody was Trueblot anti-mouse IgG-HRP (1:1,000) and Trueblot anti-rabbit IgG-HRP (1:1,000) from eBioscience. The density of protein bands was quantified by the use of ImageJ.

Protein Deglycosylation. *N*-Glycanase PNGase F (Prozyme) was used to remove the *N*-linked glycosylated sugars. Thirty-five microliters protein or IP beads suspension was sequentially mixed with 10 μL 5× Reaction Buffer (Prozyme), 2.5 μL Denaturation Solution (Prozyme), 2.5 μL Detergent Solution (Prozyme) and 1 μL PNGase F (2.5 units/mL) and then incubated at 37 °C for 1 h. For PNGase F (–) control, every component but the glycanase was included in the reaction.

Cell Surface Biotinylation. EZ Link Sulfo NHS-SS-biotin (Pierce) was used to determine the expression of HA-tagged LRRC52 on the plasma membrane of oocytes. 50 oocytes were injected with appropriate amounts of cRNA of *Slo3*, *lrrc52-HA* or *Slo3+lrrc52-HA* and incubated for 6 d in a 16 °C incubator. Before biotin labeling, oocytes were equally divided into two Petri dishes and washed once for 10 min with 4 °C ND96 oocyte culture solution. 25 oocytes in biotin(+) dish were incubated in 5 mL NHS-SS-biotin solution (0.5 mg/mL in ND96 solution) at room temperature for 30 min and then at 4 °C for 1.5 h to label the cell surface proteins. As negative controls, 25 oocytes in biotin(–) dish were incubated in 5 mL ND96 solution without biotin. After labeling, the oocytes were washed twice with 5 mL quenching buffer (50 mM glycine in PBS) to scavenge the unreacted biotin, followed by 10-min rinse with 5 mL ND96 solution four times. Total proteins were prepared from the biotin(+) and biotin(–) oocytes, mixed with 35 μL Streptavidin agarose (Prozyme) and then incubated for overnight in 4 °C cold room. Agarose beads were then collected by a brief spin and washed thrice with 1 mL lysis buffer (containing 1% Triton X-100). Biotin-labeled cell surface proteins were eluted from the streptavidin agarose with 70 μL SDS loading buffer.

ACKNOWLEDGMENTS. We thank Robert Brenner (University of Texas Health Science Center at San Antonio) for providing the *kcnmb4*$^{-/-}$ mice and Dr. Jiusheng Yan for his suggestions and interest during this project. Work was supported in part by National Institutes of Health (NIH) Grant GM081748 (to C.L.). The monoclonal antibody N2/16 was developed by or obtained from the University of California Davis/NIH NeuroMab Facility, supported by NIH Grant U24NS050606, and maintained by the Department of Neurobiology, Physiology, and Behavior, College of Biological Sciences, University of California Davis.

1. Navarro B, Kirichok Y, Clapham DE (2007) KSper, a pH-sensitive K^+ current that controls sperm membrane potential. *Proc Natl Acad Sci USA* 104:7688–7692.
2. Schreiber M, et al. (1998) Slo3, a novel pH-sensitive K^+ channel from mammalian spermatocytes. *J Biol Chem* 273:3509–3516.
3. Santi CM, et al. (2010) The SLO3 sperm-specific potassium channel plays a vital role in male fertility. *FEBS Lett* 584:1041–1046.
4. Zeng XH, Yang C, Kim ST, Lingle CJ, Xia XM (2011) Deletion of the Slo3 gene abolishes alkalization-activated K^+ current in mouse spermatozoa. *Proc Natl Acad Sci USA* 108: 5879–5884.
5. Zhang X, Zeng X-H, Lingle CJ (2006) Slo3 K^+ channels: Voltage and pH dependence of macroscopic currents. *J Gen Physiol* 128:317–336.
6. Zhang X, Zeng X-H, Xia X-M, Lingle CJ (2006) pH-regulated Slo3 K^+ channels: Properties of unitary currents. *J Gen Physiol* 128:301–315.
7. Yan J, Aldrich RW (2010) LRRC26 auxiliary protein allows BK channel activation at resting voltage without calcium. *Nature* 466:513–516.
8. Dolan J, et al. (2007) The extracellular leucine-rich repeat superfamily; A comparative survey and analysis of evolutionary relationships and expression patterns. *BMC Genomics* 8:320.
9. Yang CT, Zeng XH, Xia XM, Lingle CJ (2009) Interactions between beta subunits of the KCNMB family and Slo3: Beta4 selectively modulates Slo3 expression and function. *PLoS ONE* 4:e6135.
10. Horrigan FT, Aldrich RW (2002) Coupling between voltage sensor activation, Ca^{2+} binding and channel opening in large conductance (BK) potassium channels. *J Gen Physiol* 120:267–305.
11. Carlson AE, et al. (2003) CatSper1 required for evoked Ca^{2+} entry and control of flagellar function in sperm. *Proc Natl Acad Sci USA* 100:14864–14868.
12. Qi H, et al. (2007) All four CatSper ion channel proteins are required for male fertility and sperm cell hyperactivated motility. *Proc Natl Acad Sci USA* 104:1219–1223.
13. Liu J, Xia J, Cho KH, Clapham DE, Ren D (2007) CatSperbeta, a novel transmembrane protein in the CatSper channel complex. *J Biol Chem* 282:18945–18952.
14. Chung JJ, Navarro B, Krapivinsky G, Krapivinsky L, Clapham DE (2011) A novel gene required for male fertility and functional CATSPER channel formation in spermatozoa. *Nat Commun*,10.1038/ncomms1153.
15. Benoff S, et al. (2007) Voltage-dependent calcium channels in mammalian spermatozoa revisited. *Front Biosci* 12:1420–1449.
16. Yuan A, et al. (2003) The sodium-activated potassium channel is encoded by a member of the Slo gene family. *Neuron* 37:765–773.
17. Bhattacharjee A, et al. (2003) Slick (Slo2.1), a rapidly-gating sodium-activated potassium channel inhibited by ATP. *J Neurosci* 23:11681–11691.
18. Yuan P, Leonetti MD, Pico AR, Hsiung Y, MacKinnon R (2010) Structure of the human BK channel Ca^{2+}-activation apparatus at 3.0 A resolution. *Science* 329:182–186.